Nano Energy (▮▮▮▮) ▮, ▮▮▮–▮▮▮

Available online at www.sciencedirect.com

ScienceDirect

journal homepage: www.elsevier.com/locate/nanoenergy

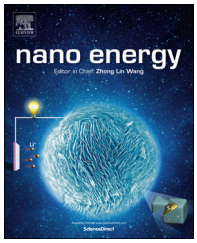

COMMUNICATION

Tuning structural stability and lithium-storage properties by *d*-orbital hybridization substitution in full tetrahedron Li_2FeSiO_4 nanocrystal

Jinlong Yang[a,b], Jiaxin Zheng[a], Xiaochun Kang[b], Gaofeng Teng[a], Lin Hu[b], Rui Tan[a], Kai Wang[a], Xiaohe Song[a], Ming Xu[a], Shichun Mu[b], Feng Pan[a]

[a]*School of Advanced Materials, Peking University Shenzhen Graduate School, Shenzhen 518055, PR China*
[b]*State Key Laboratory of Advanced Technology for Materials Synthesis and Processing, Wuhan University of Technology, Wuhan 430070, PR China*

Received 18 September 2015; received in revised form 4 December 2015; accepted 10 December 2015

KEYWORDS
Optimized Ti substitution;
d-Orbital hybridization;
Full tetrahedron Li_2FeSiO_4 nanocrystal;
Structural stability;
Lithium-storage properties

Abstract
Full tetrahedron connected structures possess considerable potential as cathodes for lithium-ion batteries (LIBs) due to more lithium storage sites to obtain high specific capacity. However, different from the full octahedron and octahedron/tetrahedron hybrid structures with coplanar or collinear, the tetrahedron network is connected by common vertex, which provokes structural instability and poor electrochemistry performance. Here, using first principles calculations combined with experiments, we found that a heavy distortion and big volume expansion during delithiation for full tetrahedron (LiO_4, FeO_4 and SiO_4 tetrahedra) Li_2FeSiO_4 nanocrystal lead to phase change or even structure fracture, and the optimized Ti(IV) doped in Fe sites can enhance the coupling effect among the tetrahedra by the strong *d*-orbital hybridization and like "spring" to hold these tetrahedra and prohibit structure fracture. Meanwhile, the Ti(IV) doping can also shorten the distance of two adjacent Li sites to decrease the activation barrier for Li-ion diffusion. Furthermore, the n-type doping effect increases the electronic conductivity. This discovery can be extended to other tetrahedron structures as well, providing a general approach to develop promising next-generation cathode materials for high-energy and long-life lithium-ion batteries.

http://dx.doi.org/10.1016/j.nanoen.2015.12.004
2211-2855/

Please cite this article as: J. Yang, et al., Tuning structural stability and lithium-storage properties by *d*-orbital hybridization substitution in full tetrahedron Li_2FeSiO_4 nanocrystal, Nano Energy (2015), http://dx.doi.org/10.1016/j.nanoen.2015.12.004

Introduction

Up to date, the most widely used/commercialized cathode materials for LIBs based on inorganic compounds mainly include layered structure [1], spinel structure [2] and polyanion structure [3]. According to the bonding model of transition metal with oxygen, these structures can be classified into the full octahedron, full tetrahedron as well as octahedron/tetrahedron hybrid structures. Compared with the full octahedron (such as layered $LiMO_2$ (M=Ni, Co and Mn)) [1] and octahedron/tetrahedron hybrid structures (such as spinel $LiMn_2O_4$ [2] and olivine $LiFePO_4$ [3a-c]), the full tetrahedron structures possess considerable potential due to that more lithium can be embedded into the tetrahedron network to obtain high specific capacity, such as Li_2MSiO_4 (M= Fe, Co and Mn) materials [4], in which two lithium ions could be embedded, corresponding to the theoretical capacity of 333 mAh/g. However, different from the full octahedron and octahedron/tetrahedron hybrid structures with coplanar or/and collinear, the tetrahedra are linked into a network by corner-sharing in full tetrahedron structures [5]. This kind of weak link can provoke the structural instability and poor electrochemistry performance of cathodes for LIBs. For example, Li_2MSiO_4 (M= Fe, Co and Mn) materials possess poor electronic conductivity and lithium diffusion as well as amorphization during charge-discharge operation [4c-f,6]. The commonly used carbon coating cannot change the intrinsic properties of such materials [7]. The intrinsic substitution using optimized atoms may be an effective approach and should be employed. But what and how substitution can play a positive role for the structure stability, the electronic conductivity and Li-ion diffusion coefficient in cathode materials for LIBs? Consequently, a detailed in-depth study is needed, which would share some clues to select appropriate elements as substitution to enhance the structure stability and electrochemistry activity of full tetrahedron structural materials.

Herein, we found that a heavy distortion and the big volume expansion during delithiation in full tetrahedron (LiO_4, FeO_4 and SiO_4 tetrahedra) Li_2FeSiO_4 nanocrystal lead to phase change or even structure fracture to become the amorphous, and we systematically studied the Ti or Sn doping-effect in full tetrahedron (LiO_4, FeO_4 and SiO_4 tetrahedra in Li_2FeSiO_4) networks [the composition and structure characteristics of these materials are shown part 1 (Figure S1-10) and part 3 (Figure S17-19) in SI]. It was prove that the structure stability and electrochemistry activity of full tetrahedron Li_2FeSiO_4 nanocrystal can be enhanced by optimized Ti(IV) substitution, mainly resulting from the strong orbital hybridization between Ti (3d and 4s orbitals) and O (2p orbital). The Ti(IV) doped in Fe sites can enhance the coupling effect among the tetrahedra and acts like "spring" to hold these tetrahedra and fix the loose structure and prohibit the structure phase change or structure cracking.

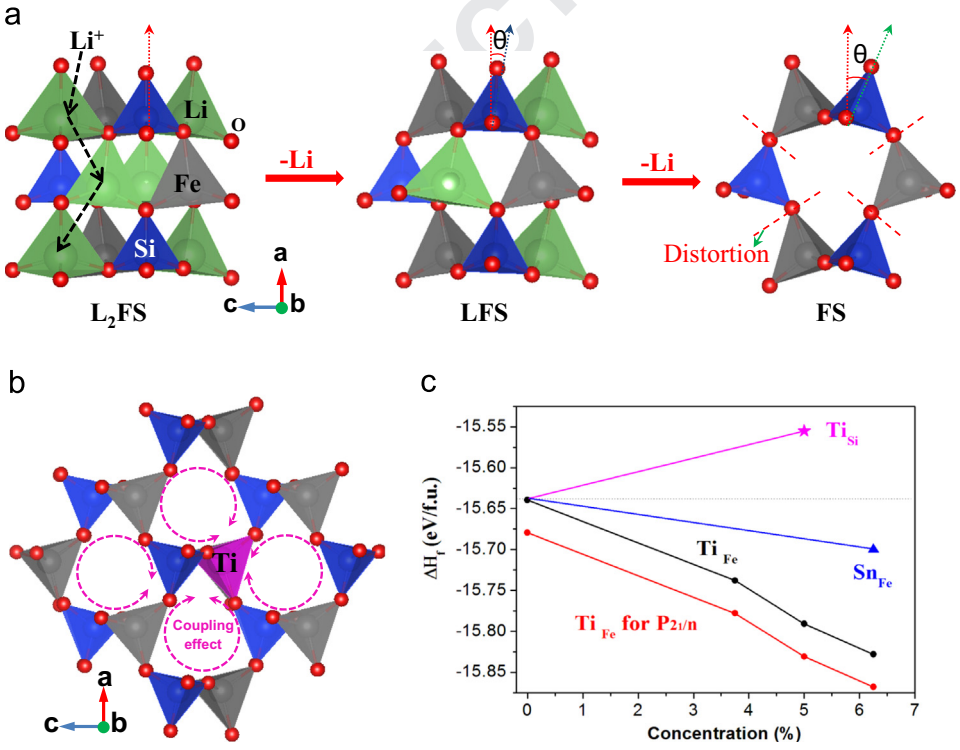

Figure 1 First-principles calculated structure properties for the cycled Li_2FeSiO_4 (L_2FS, inversed Pmn21) with and without Ti doping. (a) Full relaxed configuration for the cycled Li_2FS, half- ($LiFeSiO_4$ (LFS)) and fully- ($FeSiO_4$ (FS))delithiated structures, the dominant Li-ion diffusion path in the cycled Li_2FS and a heavy distortion lead to the structure phase change or even structure fracture in the fully-delithiated structures, (b) the structural representation of the fully-delithiated structures by Ti atoms with *d*-orbit substituted at Fe sites, the four "pink cycles" mean strong coupling effect among the TiO_4, FeO_4 and SiO_4 tetrahedra, (c) calculated formation enthalpy of Ti and Sn doped Li_2FeSiO_4. Ti_{Fe}, Ti_{Si}, and Sn_{Fe} mean Ti doping at Fe sites, Si sites, and Sn doping at Fe sites. Except for the red data ($P2_1/n$), all the left data are for doped inversed $Pmn2_1$ Li_2FeSiO_4. (For interpretation of the references to color in this figure legend, the reader is referred to the web version of this article.)

Please cite this article as: J. Yang, et al., Tuning structural stability and lithium-storage properties by *d*-orbital hybridization substitution in full tetrahedron Li_2FeSiO_4 nanocrystal, Nano Energy (2015), http://dx.doi.org/10.1016/j.nanoen.2015.12.004

Table 1 The variation of lattice parameters and volume for undoped and 5% Ti-doped cycled Li_2FeSiO_4 after half- and fully-delithiation.

	a (Å)	b (Å)	c (Å)	V (Å^3)	ΔV (V)
Li_2FeSiO_4	5.0228	5.4928	6.2675	172.915	0
$LiFeSiO_4$	5.0813	5.2295	6.6996	178.028	2.96%
$FeSiO_4$	5.3782	5.4174	7.4843	218.067	26.11%
$Li_2Fe_{0.095}Ti_{0.05}SiO_4$	5.0158	5.5028	6.2719	173.112	0
$LiFe_{0.095}Ti_{0.05}SiO_4$	5.0854	5.2163	6.7396	178.787	3.28%
$Fe_{0.095}Ti_{0.05}SiO_4$	5.3828	5.4236	7.4919	218.728	26.35%

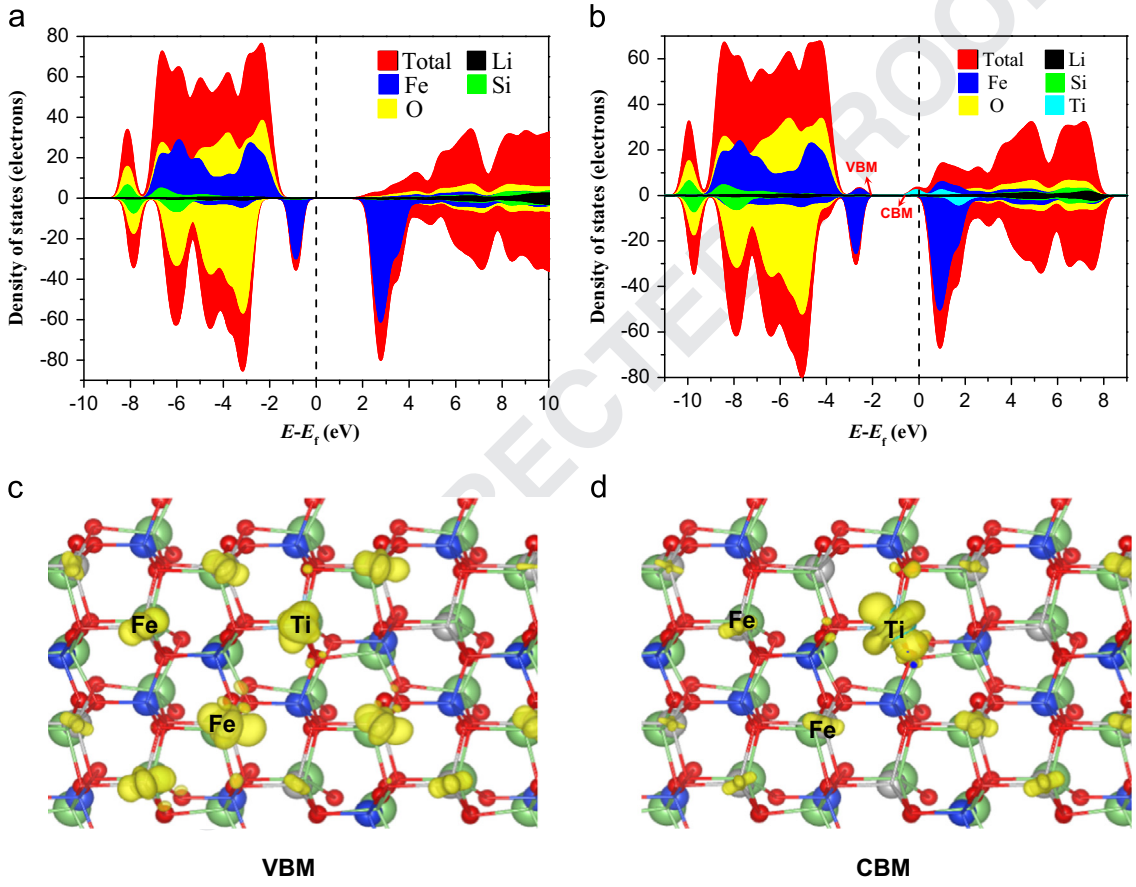

Figure 2 Calculated total and projected density of states for (a) the pristine and (b) Ti doped (5% concentration) inversed-Pmn2$_1$ Li_2FeSiO_4, the Fermi level is set to zero. (c) and (d) electron density of states, showing the valence band maximum (VBM) and conduction band minimum (CBM) levels for the Ti-doped inversed-Pmn2$_1$ Li_2FeSiO_4.

Meanwhile, the Ti(IV) can also shorten the distance of two adjacent Li sites to decrease the activation barrier for Li-ion diffusion. Finally, the n-type doping effect and the reduced band gap of full tetrahedron silicate network induced by Ti(IV) doping would increase the electrical conductivity. All these theoretical predictions were further confirmed by our experiments. A remarkable enhancement of capacity, high current-rate performance, and cycling stability for Ti doped full tetrahedron silicate LIBs were observed. This discovery can be extended to other tetrahedron structures as well.

Calculations and experiments

Calculation method

DFT calculations are performed using the plane-wave projector-augmented wave method [8], as implemented in the Vienna *ab initio* simulation package [9]. The Perdew-Burke-Ernzerhof (PBE) [10] form of generalized gradient approximation (GGA) is chosen as the exchange-correlation potential. Structural properties and electronic properties are

Please cite this article as: J. Yang, et al., Tuning structural stability and lithium-storage properties by *d*-orbital hybridization substitution in full tetrahedron Li_2FeSiO_4 nanocrystal, Nano Energy (2015), http://dx.doi.org/10.1016/j.nanoen.2015.12.004

calculated by the PBE+U approach [11], with a U=4 eV on Fe 3d states. To obtain reliable optimized structures, the maximum residual force is less than 0.01 eV/Å and energies are converged to within 5×10^{-6} eV per atom, and the k-point mesh is set to $9 \times 9 \times 9$ ($2 \times 2 \times 1$ supercell). An energy cut-off of 400 eV was used in all cases. A climbing-image nudged elastic band (cNEB) method [12] is employed to calculate the energy barriers for Li-ion diffusion in the dominant Li-ion transport path in Li_2FeSiO_4.

Synthesis and structural characterizations

In the typical sol-gel synthesis procedure, 0.03 mol of $CH_3COOLi \cdot 2H_2O$, 0.015 mol of $Fe(NO_3)_3 \cdot 9H_2O$ were separately dissolved in 30 ml of deionized water and 0.015 mol of tetraethyl orthosilicate (TEOS) was dissolved in 20 mL ethyl alcohol, then stirred together to form a homogeneous solution. After that, 0.015 mol of citric acid was added drop-by-drop to the homogeneous solution. The end solution was stirred at 70 °C in water bath for 10 h and then dried in an oven at 80 °C for 24 h. The dry material was calcined at 650 °C for 10 h under argon atmosphere. For the sample of $Li_2Fe_{1-x}Ti_xSiO_4$ and $Li_2Fe_{1-x}Sn_xSiO_4$, we added tetrabutyl titanate (TBT) and stannous sulphate ($SnSO_4$) in the above homogeneous solution, and the regents in the solution were stoichiometric depend on the x. All chemical regents and solvents in this experiment were of analytical grade and used without further purification.

Table 2 Fermi level (ΔE_f) and band gap (E_g) with the Ti doping content increasing from x=0.0% to x=6.25%.

	Li_2FeSiO_4	3.75% Ti	5% Ti	6.25% Ti
ΔE_f	0	1.83	1.86	1.92
E_g	2.13	1.68	1.46	1.50

The morphologies of the samples were investigated using field-emission scanning electron microscopy (FE-SEM, Hitachi S-4800, 10 kV) and high-resolution transmission electron microscopy (HRTEM, JEM-2100F, 200 kV). The chemical compositions of the samples were analyzed using energy-dispersive X-ray spectroscopy (EDX, Horbia EX-250, 20 kV) as well as FE-SEM and Fourier-transform infrared spectroscopy (FTIR, Nicolet Avatar 360). The crystalline structures of the samples were determined via X-ray diffraction (XRD, D/MAX-IIIA, Cu Kα radiation, λ=0.15406 nm). The specific surface area and pore size distribution were analyzed via Brunauer–Emmett–Teller (BET) nitrogen adsorption-desorption measurements (Japan, BELSORP-Mini). The Raman spectra were obtained using an RM-1000 Renishaw confocal

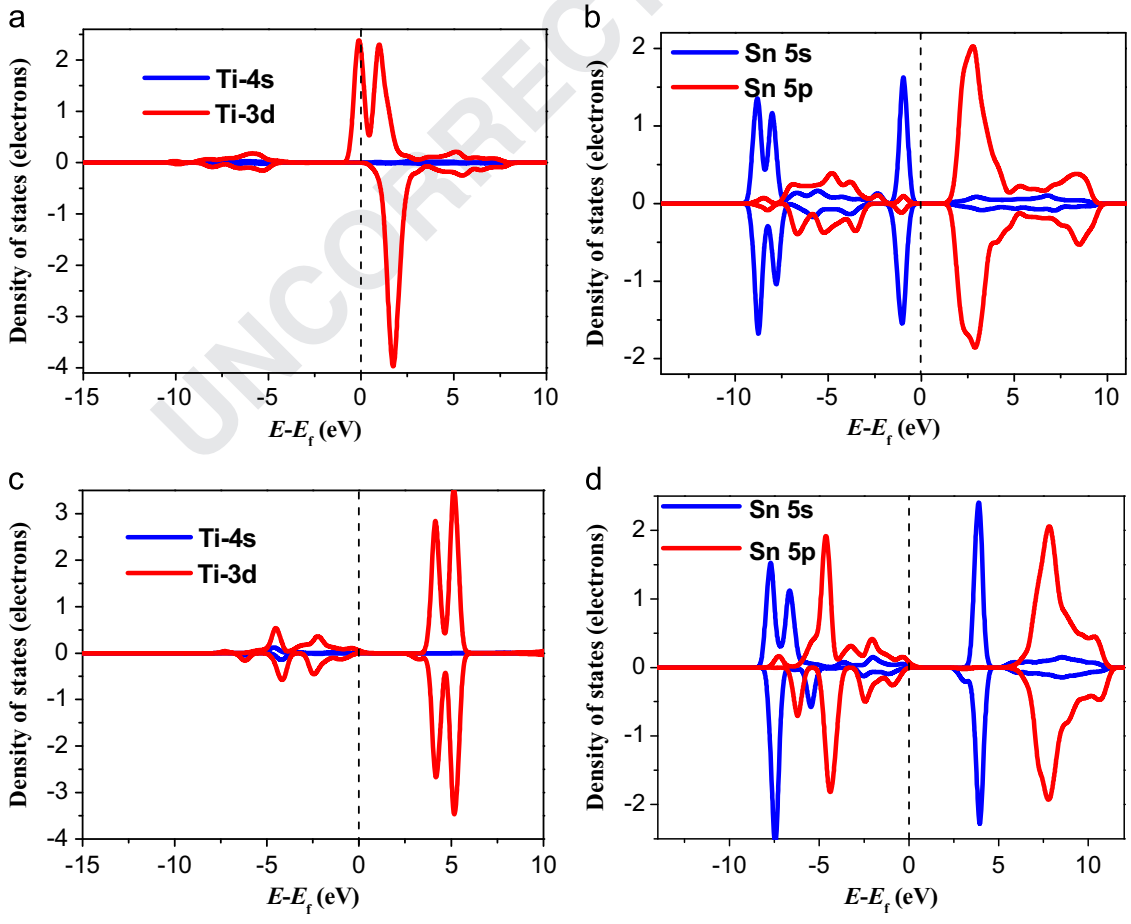

Figure 3 Projected density states (PDOS) of (a) Ti orbitals and (b) Sn orbitals in the Ti- and Sn-doped (at Fe sites) inversed-Pmn2$_1$ Li_2FeSiO_4, respectively; PDOS for (c) Ti orbitals and (d) Sn orbitals after delithiation.

Please cite this article as: J. Yang, et al., Tuning structural stability and lithium-storage properties by *d*-orbital hybridization substitution in full tetrahedron Li_2FeSiO_4 nanocrystal, Nano Energy (2015), http://dx.doi.org/10.1016/j.nanoen.2015.12.004

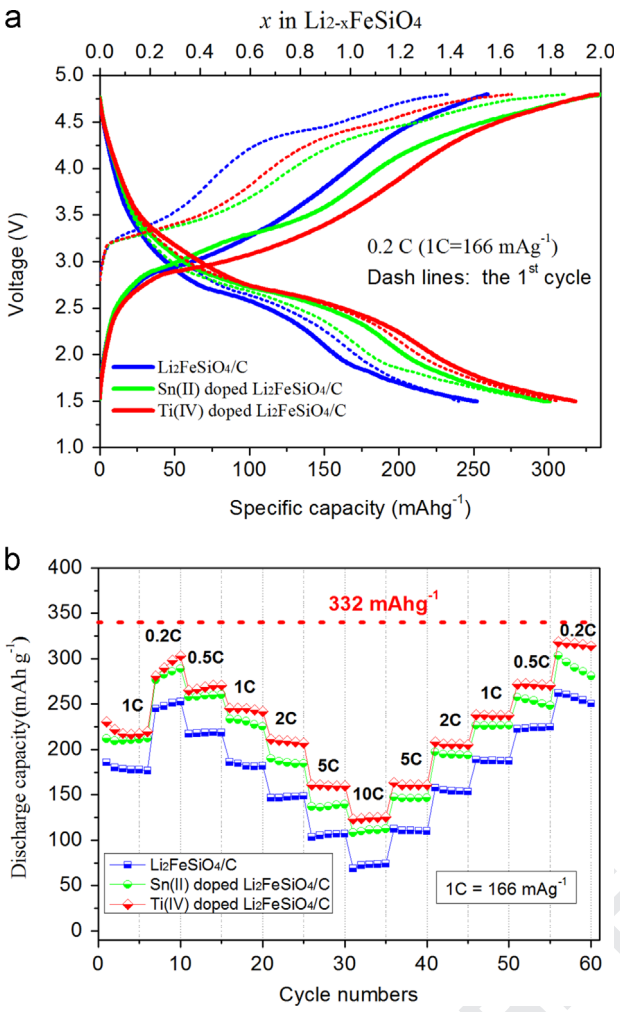

Figure 4 Electrochemical properties of the samples as cathode materials for lithium ion batteries: (a) typical galvanostatic charge-discharge curves at 0.2 C (1 C=166 mA g^{-1}), (b) rate capability from 0.2 to 10 C for 5% Ti or Sn doped and pristine Li_2FeSiO_4 samples.

Raman microspectroscope with 514.5 nm laser radiation at a laser power of 0.04 mW in the range of 200–3000 cm^{-1}.

Electrochemical measurements

The electrochemical properties were tested with 2032-type coin cells assembled in a glove box filled with pure argon. Lithium pellets were used as the anodes, a 1.0 M solution of $LiPF_6$ in ethylene carbonate/dimethyl carbonate (1/1) (bought from Shenzhen new main bond technology co., LTD. China) was used as the electrolyte, and the cathode electrodes were produced with 75% active material, 15% conducting agent (Ketjen Black) and 10% poly(tetrafluoroethylene) binder. Galvanostatic charge/discharge measurement was performed in the potential range from 1.5 to 4.8 V vs. Li/Li^+ with a multichannel battery testing system (LAND CT2001A) at room temperature. Cyclic voltammetry (CV) and Alternating-current impedance (AC) Nyquist measurements were performed using an electrochemical workstation (CHI 760D).

Results and discussion

Theoretical calculations

Based on the previous studies [5,13], multiple phase transformation happens from the initially prepared phase ($P2_1/n$ for prepared-Li_2FeSiO_4) to cycling stable phase (inversed-$Pmn2_1$) during the initial charge and discharge processes. The same structure change also appears in the Ti and Sn substitution structures (Figure S11 and S20). Here we mainly focused on the cycling stable inversed-$Pmn2_1$ structure.

Structural stability

One problem that limits the performance of full tetrahedron silicate networks (LiO_4, FeO_4 and SiO_4 tetrahedra in Li_2FeSiO_4) is the poor structure stability due to large volume change during delithiation and lithiation. Even for the cycled structure (inversed-$Pmn2_1$), our calculation results show there is a significant structure change after the full extraction of Li-ions. Figure 1a shows the optimized structures of the inversed $Pmn2_1$ Li_2FeSiO_4 (L_2FS), $LiFeSiO_4$ (LFS), and $FeSiO_4$ (FS). In the inversed $Pmn2_1$ L_2FS, all the Li, Fe, and Si cations are in tetrahedral sites pointing in the same direction along *b*, and all tetrahedra are linked only by corner-sharing. During the extraction of Li-ions, due to the transformation of the valence state of Fe, the size of FeO_4 tetrahedra is reduced, and the size of SiO_4 tetrahedra is also reduced a little (the average Si-O bond decreases from 1.658 Å to 1.633 Å). In principle, the size reduced FeO_4 tetrahedra and SiO_4 tetrahedra would lead to the volume shrinkage. However, the reduced FeO_4 tetrahedra would also lead to the strong pulling among all the FeO_4 and SiO_4 tetrahedra and the significant tilt of them along the *b* direction. Figure 1a shows that the FeO_4 and SiO_4 tetrahedra are rotated by a degree of θ along ***a*** axis. With the extracted Li-ions increase, the θ increases, thus resulting in a heavy structure distortion. This structure distortion becomes much heavier after the extraction of the second Li: the θ was up to maximum, *a* and *c* lattices expand by 7.1% and 19.4%, respectively, and *b* shrinks by 1.4% after the full Li-ion extraction (Table 1). The final volume expansion reaches up to 26.11% for the full-delithiated $FeSiO_4$. The heavy distortion and the big volume expansion finally produce strong stresses between the FeO_4 and SiO_4 tetrahedra, which lead to the structure phase change or even structure fracture to become the amorphous.

To study the thermodynamic stability after Ti doping, we first calculated its formation energy (enthalpy) for both initially prepared $P2_1/n$ phase and cycled phase. Figure 1b shows the doping model of Fe substituted by Ti. The formation energy of Ti doping at Fe sites ($Li_2Fe_{1-x}Ti_xSiO_4$) is defined as

$$\Delta H_f = E_{tot}^{Li_2Fe_{(1-x)}Ti_xSiO_4} - 2E_{crystal}^{Li} - (1-x)E_{crystal}^{Fe} - xE_{crystal}^{Ti} - E_{crystal}^{Si} - 2E_{gas}^{O_2}$$

where $E_{tot}^{Li_2Fe_{(1-x)}Ti_xSiO_4}$ is the total energy of Ti doped Li_2FeSiO_4, $E_{crystal}^{Li}$, $E_{crystal}^{Fe}$, $E_{crystal}^{Ti}$, and $E_{crystal}^{Si}$ are Li, Fe, Ti, and Si at their most stable phases, $E_{gas}^{O_2}$ is the energy of O_2 molecular gas, respectively. For each *x* value, we have considered at least four substitution structures and found out that the uniform doping is the most energy stable

Please cite this article as: J. Yang, et al., Tuning structural stability and lithium-storage properties by *d*-orbital hybridization substitution in full tetrahedron Li_2FeSiO_4 nanocrystal, Nano Energy (2015), http://dx.doi.org/10.1016/j.nanoen.2015.12.004

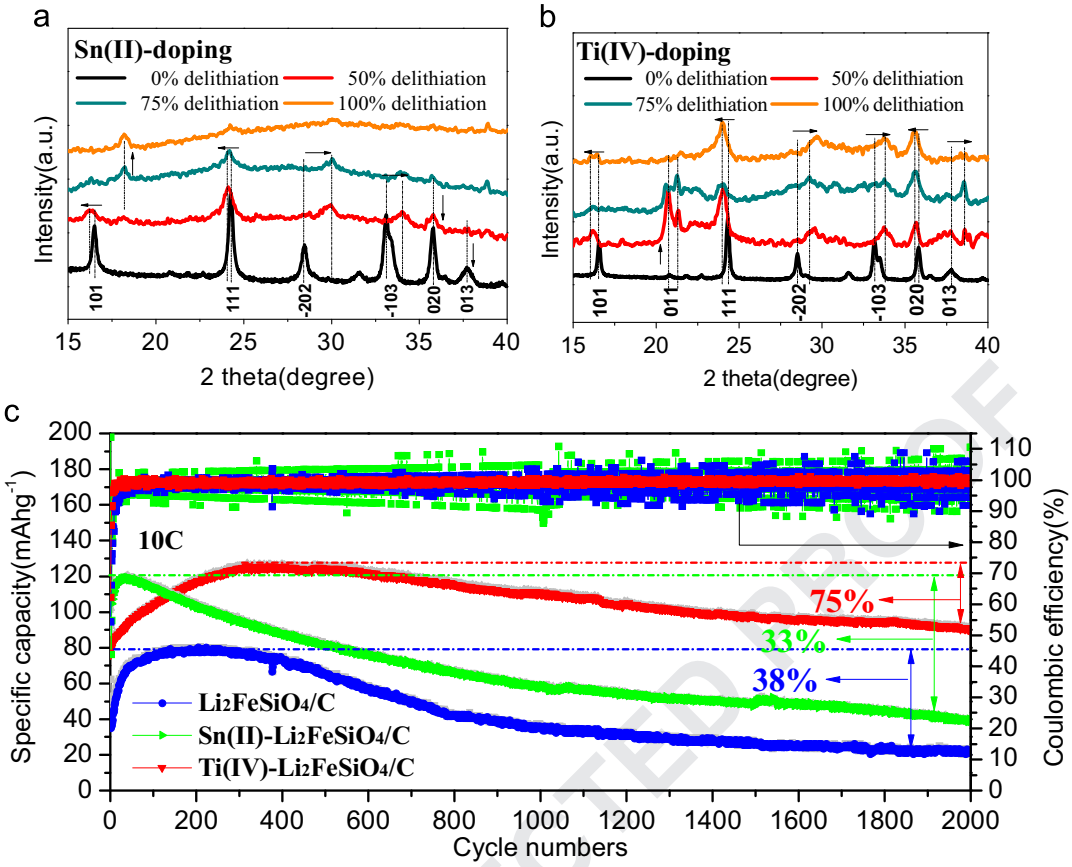

Figure 5 Structure stabilities of the 5% Ti or Sn doped and pristine Li_2FeSiO_4 samples: XRD patterns for (a) Sn and (b) Ti doped samples with different delithiation, (c) cycling performance at 10 C for pristine, 5% Sn and Ti substituted samples.

doping style. The calculated formation energies under different doping concentrations for both $P2_1/n$ and inversed $Pmn2_1$ phases are shown in Figure 1c. For comparison, we also calculated Ti doping at Si sites and Sn doping at Fe sites for the inversed $Pmn2_1$ structure at fixed concentrations, respectively. We can see that for the Ti doping at Fe sites for both phases, the ΔH_f decreases with the doping concentration, indicating the enhanced structure stability. The Ti atom enhances the coupling effect among the tetrahedra and acts like a spring to hold SiO_4 tetrahedra and further hold FeO_4 tetrahedra around it through its four vertexes (Ti-O-(Si-O-Fe-) bonds) (Figure 1b), as discussed in the following part. Sn doping at Fe sites can also enhance the structure stability but with much smaller degree than the Ti doping. By contrast, Ti doping at Si sites decreases the structure stability with an increased ΔH_f.

Lithium-ion diffusion

Furthermore, lattices of *b*, *c*, and the total volume *V* increase but lattice *a* decreases a little after the Ti doping at the Fe sites, and the Fe-O, Si-O, and Li-O bonds also increases a little after the Ti doping (Table S2). After the full extraction of Li-ions, the lattices *a* and *c* expand by 7.3% and 19.45%, respectively, and *b* shrinks by 1.4% after the full Li-ion extraction (Table 1), nearly the same structure change as the undoped Li_2FeSiO_4. According to previous literatures and our previous calculations [4-6], there is one dominant Li-ion diffusion path with an activation barrier of 0.82 eV for the inversed $Pmn2_1$ Li_2FeSiO_4: the path along the *a*-axis direction with zigzag paths between corner-sharing Li_1 and Li_2 sites and through intervening vacant octahedral sites that share faces with the LiO_4 tetrahedral (L_2FS in Figure 1). Thus the *b* and *c* expansion after Ti doping would enlarge the size of Li migration path to decrease the activation barrier, and the ***a*** shrinkage after Ti doping also shortens the distance of two adjacent Li sites to decrease the activation barrier. To confirm this, we calculated the activation barrier for Li-ion diffusion in the dominant path after Ti doping, and the calculated value is 0.74 eV, which is lower than that of undoped Li_2FeSiO_4. Therefore, the Li-ion diffusion in Li_2FeSiO_4 can be facilitated by Ti doping, which are also revealed by the improved Li-ion diffusion coefficient from the results of the fitting of EIS at low frequency (Figure S13) as well as the decreased activation energies (E_a) (Figure S14 and Table S4 in SI).

Electronic conductivity

The electronic properties after Fe substituted with Ti were further calculated. Different Ti doping levels of 3.75%, 5%, and 6.25% were considered, and the plotted density of states (DOS) are shown in Figure 2. The calculated band gap for the cycled Li_2FeSiO_4 is 2.13 eV, same as the calculated value in Materials Project. From Figure 2a and b, our calculation clearly revealed a shift of the Fermi level toward and crossing the conduction band with Fe substituted by Ti. The Fermi level shift reaches up to 1.92 eV with

Please cite this article as: J. Yang, et al., Tuning structural stability and lithium-storage properties by *d*-orbital hybridization substitution in full tetrahedron Li_2FeSiO_4 nanocrystal, Nano Energy (2015), http://dx.doi.org/10.1016/j.nanoen.2015.12.004

the Ti doping content increasing from $x=0.0$ to $x=0.0625$ (Table 2). This upward shift to the conduction band for the Fermi level indicates an *n*-type doping effect when Fe substituted by Ti for the cycled Li_2FeSiO_4, which is attributed to that the heterovalent substitution of Fe atoms by Ti atoms introduces extra electrons in the conduction band (Figure 2b). The *n*-type doping effect will increase the electron concentration and contribute to the electrical conductance. Moreover, the band gap (E_g) is also narrowed when the Fe atoms are substituted by the Ti atoms: the band gap is first narrowed from 2.13 eV to 1.69 eV with the content of Ti doping increased from 0 to 3.75% and then further to 1.46 eV with the doping content increased to 5% (Table 2). But when the Ti doping content is further increased to 6.25%, the band gap is enlarged a little by 0.04 eV compared with the case of 5% Ti doping. The narrowed band gap can be attributed to the decreased interaction between Fe/Li and O atoms after Ti doping and *d*-orbital contribution at the CBM from Ti and would improve the electrical conductivity of Li_2FeSiO_4. The increased electrical conductivity was revealed by our EIS experiments (Figure S12 and Table S3) and supported the improvement of electrochemical properties with optimum Ti doping content (Figure S15–16 in SI).

What mechanism results in the structure stability and enhanced electrochemical activity after Ti doping? For undoped Li_2FeSiO_4, the VBM and CBM are mainly composed of $3d_{Fe}$ orbitals (Figure 2a). After doping with Ti atoms, the $3d_{Ti}$ orbitals contribute to the CBM (Figs. 2b, 3a). Figure 2c and d shows the electron DOS of the VBM and CBM levels for the Ti-doped cycled Li_2FeSiO_4, and we can see that the DOS of the VBM are mainly distributed around Fe atoms and the DOS of the CBM are mainly distributed around Ti atoms. There is a strong orbital hybridization between Ti (3d orbital) and O (2p orbital), leading to the +4 valence state for Ti (Figure 3a). However, here the valence state of Ti is not total +4 but $+x$ ($3<x<4$), because partial DOS of 3d orbitals of Ti is still under the Fermi level and occupied with electrons (Figure 3a). These extra unbonded electrons would become delocalized (e.g., being transferred a little partial to Fe atoms) and contribute to the electrical conductance of the cycled Li_2FeSiO_4. On the other hand, for charge compensation, the interaction between other cations (Fe, Li, and Si) and oxygen will decrease, which is evidenced by the increased Fe-O, Si-O, and Li-O bond lengths after Ti doping (Table S2). During the delithiation process, the Ti^{x+} will be first oxidized to Ti^{4+} at the initial stage (Figure 3c), and this nearly invariance for the valence state of Ti would keep the size of TiO_4 tetrahedra nearly unchanged after the Li extraction. Thus, the Ti-doping acts like "nailing" to fix the loose full tetrahedral structures to enable the structure stability of Li_2FeSiO_4. In contrast, for the Sn doping (containing two 5s and two 5p electrons) at Fe sites, we can see that Sn exhibits +2 valence state (Figure 3b). There is an orbital overlap between Sn 5p orbitals and oxygen 2p states, but the Sn 5s orbitals are occupied. So the orbital hybridization between Sn (5s and 5p orbital) and O (2p orbital) is much weaker than that between Ti and O. Moreover, the Sn^{2+} will be first oxidized to Sn^{4+} at the initial stage of delithiation (Figure 3d and also revealed by the Sn 3d 5/2 banding energy for Sn doped samples with delithiation in Figure S21), thus leading to the huge shrinkage of the size of SnO_4 tetrahedra, which is not beneficial to the structure stability of Li_2FeSiO_4.

Electrochemical properties

To finally evaluate the electrochemical properties of the samples as cathode materials for lithium ion batteries, galvanostatic charge-discharge measurements at room temperature were carried out with lithium cells over a potential window of 1.5-4.8 V (vs. Li^+/Li). Specially, the silicate cathode needs to carry out a structural rearrangement from an initial $P2_1/n$-structure to cycled invest-$Pmn2_1$ structure arousing different lithium-ion transport process [5,13]. The different track in initial two galvanostatic charge-discharge curves (Figure 4a) suggests the structural rearrangement can cause different electrochemical behavior, which can be observed in doped and undoped samples and support the dependability of theoretical calculations using cycled invest-$Pmn2_1$ structure. Observing the subsequent stable galvanostatic profiles of 5% Ti or Sn doped and pristine Li_2FeSiO_4/C cathodes at 0.2 C (1 C=166 mA g^{-1}) in Figure 4a, the pristine Li_2FeSiO_4 performed discharge specific capacity of 250 mAh g^{-1} at 0.2 C, corresponding to 1.5 Li-ion storages in Li_2FeSiO_4. This result is similar to that of the most reported nano-Li_2FeSiO_4/C materials, confirming that the nanotechnology is a good way to promote more than one Li-ion store in silicate cathodes [14,15]. The Ti (or Sn) doped Li_2FeSiO_4/C performed discharge specific capacity of 317 (or 305) mAh g^{-1}, which approached the theoretical capacity with two Li-ion storages per Li_2FeSiO_4 formula unit, indicating a preferable way of metallic doping in silicate nanocrystalline to increase discharge capacity. Figure 4b further compares the rate capabilities of the three samples. Obviously, the doped samples exhibit much better rate capability than the pristine Li_2FeSiO_4. The enhanced Li-ion diffusion coefficient and electronic conductivity provide the evidences of high rate performance. But only Ti doped sample regain the 100% capacities after rate testing, the pristine and Sn doped samples show the obvious decline at 0.2 C.

The structure stability of the samples was further confirmed by delithiation structural analysis (Figure 5a and b and Figure S22). The XRD peaks shift and become broad during delithiation for all the samples, indicating a large distortion and expansion for the Li_2FeSiO_4 structure and consistent with our theoretical predicted results. The shift becomes much heavier after the second Li extraction. Clearly, we can see that the peaks also become weaker during delithiation for all the samples. For the pristine samples, there are only two peaks left after full delithiation (Figure S22), and the peaks even vanish after the full Li extraction for the Sn doped samples (Figure 5a). By contrast, nearly all the peaks still exist after full delithiation for the Ti doped samples (Figure 5b), indicating a much more stable structure for the Ti doped Li_2FeSiO_4, which confirms our theoretical predicted results. Figure 5c further illustrates the cycling performance conducted at 10 C-rate for 2000 cycles. Notably, the discharge capacities of all samples increased within different initial cycled numbers because of electrode activation process at high C-rate. After that, their discharge capacities appear to decay due to the crystal structure collapse and amorphization.

Please cite this article as: J. Yang, et al., Tuning structural stability and lithium-storage properties by *d*-orbital hybridization substitution in full tetrahedron Li_2FeSiO_4 nanocrystal, Nano Energy (2015), http://dx.doi.org/10.1016/j.nanoen.2015.12.004

Compared to the reported LFS in literature[4], the LFS nanocrystalline in this work shows the best long-term cycling stability with 2000 cycles, demonstrating the structure advantage of the composite with nanocrystalline embedded in carbon network. Furthermore, Ti doped Li_2FeSiO_4 shows better cycling stability, the total capacity retention is 75% within 2000 cycles, significantly higher than that (38%) of pristine Li_2FeSiO_4. Note that the Sn doped Li_2FeSiO_4 capacity retention is 33%, lower than that of pristine LFS. Especially, the jagged coulombic efficiency for the pristine and Sn doped Li_2FeSiO_4 further demonstrated the rapidly capacity decay mechanism. However, the Ti doped Li_2FeSiO_4 processed the coulombic efficiency of ~100% within 2000 cycles, demonstrating excellent electrochemical structural stability.

Conclusion

In summary, our results reveal significantly enhanced structure stability during cycling and improved electrical conductivity and lithium-ion diffusion coefficient in the cycled Li_2FeSiO_4 after Ti doping. Thus a remarkable enhancement of capacity (approaching theoretical capacity), a high C-rate performance and a long cycling-life are obtained in Ti doped Li_2FeSiO_4. This work demonstrates the structure stability of full tetrahedron structure material can be tuned by "nailing" with optimized substitution, such as Ti(IV) doping in Li_2FeSiO_4 with strong *d*-orbital hybridization to fix the loose structure. Such strong *d*-orbital hybridization can also enlarge the size of Li migration path and shorten the distance of two adjacent Li sites to decrease the activation barrier for Li-ion diffusion. Moreover, the n-type doping effect and the reduced band gap of Li_2FeSiO_4 induced by Ti(IV) doping would increase the electrical conductivity. The mechanism can be extended to other tetrahedron structures as well, providing a general approach to develop promising next-generation cathode materials for high-energy lithium-ion batteries.

Acknowledgments

Q5 Q4 This research was financially supported by the National Natural Science Foundation of China (No. 51372186), National Project for EV Batteries (20121110, Optimum Nano, Shenzhen), Guangdong Innovation Team Project (No. 2013N080), Shenzhen Science and Technology Research Grant (No. ZDSY 20130331145131323, CXZZ 20120829172325895, JCYJ 20120614150338154, JCYJ 20140903101633318).

Appendix A. Supplementary material

Supplementary data associated with this article can be found in the online version at http://dx.doi.org/10.1016/j.nanoen.2015.12.004.

References

[1] (a) K. Mizushima, P.C. Jones, P.J. Wiseman, J.B. Goodenough, Mater. Res. Bull. 15 (1980) 783–789;
(b) T. Ohzuku, Y. Makimura, Chem. Lett. 8 (2001) 744–745;
(c) A.R. Armstrong, P.G. Bruce, Nature 381 (1996) 499–500;
(d) K. Kang, Y.S. Meng, J. Bréger, C.P. Grey, G. Ceder, Science 311 (2006) 977–980.
[2] (a) M.M. Thackeray, W.I.F. David, P.G. Bruce, J.B. Goodenough, Mater. Res. Bull. 18 (1983) 461–472;
(b) D.H. Jang, Y.J. Shin, S.M. Oh, J. Electrochem. Soc. 143 (1996) 2204–2211.
[3] (a) A.K. Padhi, K.S. Nanjundaswamy, J.B. Goodenough J. Electrochem. Soc. 144 (1997) 1188–1194;
(b) M. Thackeray, Nat. Mater. 1 (2002) 81–82;
(c) B. Kang, G. Ceder, Nature 458 (2009) 190–193;
(d) A. Nytén, A. Abouimrane, M. Armand, T. Gustafsson J.O. Thomas, Electrochem. Commun. 7 (2005) 156–160.
[4] (a) Z.L. Gong, Y. Yang, Energy Environ. Sci. 4 (2011) 3223–3242;
(b) T. Muraliganth, K.R. Stroukoff, A. Manthiram, Chem. Mater. 22 (2010) 5754–5761;
(c) D. Rangappa, K.D. Murukanahally, T. Tomai, A. Unemoto, I. Honma, Nano Lett. 12 (2012) 1146–1151;
(d) J. Yang, L. Hu, J. Zheng, D. He, L. Tian, S. Mu, F. Pan J. Mater. Chem. A 3 (2015) 9601–9608;
(e) J. Yang, X. Kang, D. He, A. Zheng, M. Pan, S. Mu, J. Mater. Chem. A 3 (2015) 16567–16573;
(f) R. Tan, J. Yang, J. Zheng, K. Wang, L. Lin, S. Ji, J. Liu, F. Pan, Nano Energy 16 (2015) 112–121.
[5] (a) S.I. Nishimura, S. Hayase, R. Kanno, M. Yashima, N. Nakayama, A. Yamada, J. Am. Chem. Soc. 130 (2008) 13212–13213;
(b) C. Sirisopanaporn, C. Masquelier, P.G. Bruce, A.R. Armstrong, R. Dominko, J. Am. Chem. Soc. 133 (2010) 1263–1265.
[6] (a) R. Dominko, J. Power Sources 184 (2008) 462–468;
(b) R.B. Araujo, R.H. Scheicher, J.S. de Almeida, A.F. da Silva, R. Ahuja, Solid State Ion. 247 (2013) 8–14.
[7] S.Y. Chung, J.T. Bloking, Y.M. Chiang, Nat. Mater. 1 (2002) 123–128.
[8] (a) P.E. Blöchl, Phys. Rev. B 50 (1994) 17953;
(b) G. Kresse, D. Joubert, Phys. Rev. B 59 (1999) 1758–1775.
[9] (a) G. Kresse, J. Furthmüller, Phys. Rev. B 54 (1996) 11169;
(b) G. Kresse, J. Furthmüller, Comput. Mater. Sci. 6 (1996) 15.
[10] J.P. Perdew, K. Burke, M. Ernzerhof, Phys. Rev. Lett. 77 (1996) 3865.
[11] V.I. Anisimov, J. Zaanen, O.K. Andersen, Phys. Rev. B 44 (1991) 943.
[12] (a) G. Henkelman, H. Jónsson, J. Chem. Phys. 113 (2000) 9978–9985;
(b) G. Henkelman, B.P. Uberuaga, H. Jónsson, J. Chem. Phys. 113 (2000) 9901–9904;
(c) H. Guo, X. Song, Z. Zhuo, J. Hu, T. Liu, Y. Duan, J. Zheng, Z. Chen, W. Yang, K. Amine, F. Pan, Nano Lett. (2015). Q6 http://dx.doi.org/10.1021/acs.nanolett.5b04302.
[13] (a) D.H. Seo, H. Kim, I. Park, J. Hong, K. Kang, Phys. Rev. B 84 (2011) 220106;
(b) A. Nytén, S. Kamali, L. Häggström, T. Gustafsson J.O. Thomas, J. Mater. Chem. 16 (2006) 2266–2272.
[14] Z. Chen, S. Qiu, Y. Cao, J. Qian, X. Ai, K. Xie, X. Hong, H. Yang, J. Mater. Chem. A 1 (2013) 4988–4992.
[15] (a) D.M. Kempaiah, D. Rangappa, I. Honma, Chem. Commun. 48 (2012) 2698–2700;
(b) G. He, A. Manthiram, Adv. Funct. Mater. 24 (2014) 5277–5283.

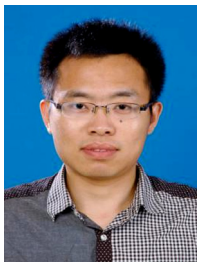

Jinlong Yang received his B. Sc in 2008 from Anhui Jianzhu University, China. Then he received his Ph. D degree in 2014 from Wuhan University of Technology. He is currently a post-doctoral fellow at School of Advanced Materials, Peking University, Shenzhen Graduate School, China. His research interests include: energy materials (battery materials, catalytic materials, carbon materials), nanomaterials, electrochemistry.

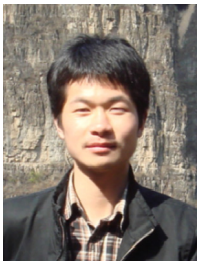

Jiaxin Zheng received his B. Sc in Physics in 2008 and Ph. D degree in Condensed Matter Physics in 2013 from Peking University, China. Then he joined the group of Prof. Feng Pan at School of Advanced Materials (SAM), Peking University, Shenzhen Graduate School, China, as a post-doctoral fellow from Oct. 2013 to Oct. 2015. Now he works an assistant Professor at SAM. His research interests include: computational materials, energy materials (battery materials, solar energy, thermoelectric materials), nanomaterials, nanoelectronics.

Xiaochun Kang received his B. Sc degree in 2011 in material Physics from Wuhan University of Technology, China. Then he joined the research group of Prof. Shichun Mu at State Key Laboratory of Advanced Technology for Materials Synthesis and Processing, Wuhan University of Technology, and received his M.Sc. degree in 2014. His research interests include: lithium ion battery materials and related devices.

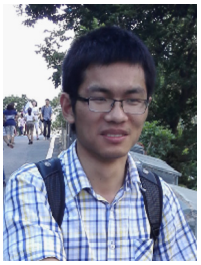

Gaofeng Teng received his B.S in 2014. He is now a student of school of Advanced Materials, Peking University, Shenzhen Graduate School, China. His research interest is on energy materials.

Lin Hu obtained his B. Sc in 2012 and M.Sc. degree in 2015 in material discipline from Wuhan University of Technology, China. Then he joined the research group of the liquid metal battery energy storage project. His research interests include: energy materials and constructional design of battery.

Rui Tan received his B. Sc degree in 2014 from Central South University, China. He is pursuing his M. Sc. degree in the School of Advanced Materials, Peking University, China. His research interests include advanced functional materials and their new application in energy storage and conversion devices, such all solid state batteries, lithium sulfur batteries and so on.

Kai Wang received his B. Sc in 2013 from Nankai University, China. He is pursuing his M.Sc. degree in the School of Advanced Materials, Peking University, China. His research interests include lithium electrode materials and their new application in energy storage and conversion devices.

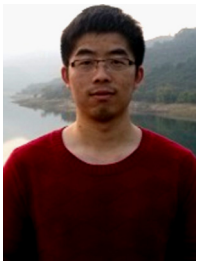

Xiaohe Song received his B.S. in Physics in 2013 from Zhengzhou University. He is now getting the Master's degree at School of Advanced Materials, Peking University, since 2013, working on energy materials using theoretical and computational methods.

Ming Xu got his B.S. in Physics in 2011 from Yanbian University. He is studying at School of Advanced Materials, Peking University, Shenzhen Graduate School, China for Master's degree, working on electrocatalysts, battery materials using theoretical and computational methods.

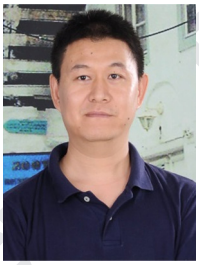

Dr. Shichun Mu is currently working as a professor at Wuhan University of Technology. He received his B.S. degree from Jilin University in 1995 and Ph.D. degree from Chinese Academy of Sciences, China in 2001. Afterwards, he joined the State Key Laboratory of Advanced Technology for Materials Synthesis and Processing, Wuhan University of Technology as a postdoctoral researcher with Prof. Runzhang Yuan (Fuel cell group), 2001–2003. He then was an associate professor and has been a full professor since 2006 at Wuhan University of Technology. He was an academic visitor at Inorganic Chemistry Laboratory, University of Oxford (2007–2008). His research focuses on nanocarbon materials, PEM fuel cell catalysts, lithium ion battery materials and related devices. He has published over 200 papers and patents.

Prof. Feng Pan, founding Dean of School of Advanced Materials, Peking University Shenzhen Graduate School, got B.S. from Dept. Chemistry, Peking University in 1985 and PhD from Dept. of P&A Chemistry,University of Strathclyde, Glasgow, UK, with "Patrick D. Ritchie Prize" for the best Ph.D. in 1994. With more than a decade experience in large international incorporations, Prof. Pan has been engaged in fundamental research and product development of novel optoelectronic and energy storage materials and devices. As Chief Scientist, Prof. Pan led eight entities in Shenzhen to win the 150 million RMB grant for the national new energy vehicles (power battery) innovation project since 2013.

Please cite this article as: J. Yang, et al., Tuning structural stability and lithium-storage properties by *d*-orbital hybridization substitution in full tetrahedron Li_2FeSiO_4 nanocrystal, Nano Energy (2015), http://dx.doi.org/10.1016/j.nanoen.2015.12.004